INTERNATIONAL JOURNAL FOR NUMERICAL METHODS IN FLUIDS, VOL. 25, 1409–1420 (1997)

NUMERICAL SIMULATION OF SHEAR EFFECT ON VORTEX SHEDDING BEHIND A SQUARE CYLINDER

ROBERT R. HWANG[1]* AND Y. C. SUE[2]

[1] *Institute of Physics, Academia Sinica, Nankang, Taipei 11529, Taiwan;* [2] *Department of Naval Architecture and Ocean Engineering, NTU, Taipei, Taiwan*

SUMMARY

This paper is concerned with the numerical simulation of the flow structure around a square cylinder in a uniform shear flow. The calculations were conducted by solving the unsteady 2D Navier–Stokes equations with a finite difference method. The effect of the shear parameter K of the approaching flow on the vortex-shedding Strouhal number and the force coefficients acting on the square cylinder is investigated in the range $K = 0{\cdot}0$–$0{\cdot}25$ at various Reynolds numbers from 500 to 1500. The computational results are compared with some existing experimental data and previous studies. The effect of shear rate on the Strouhal number and the force acting on the cylinder has a tendency to reduce the oscillation. The Strouhal number, mean drag and amplitude of the fluctuating force tend to decrease as the shear rate increases, but show no significant change at low shear rate. Increasing the Reynolds number decreases the Strouhal number and increases the force acting on the cylinder. At high shear rate the shedding frequencies of the fluctuating drag and lift coefficients are identical. © 1997 John Wiley & Sons, Ltd.

Int. J. Numer. Meth. Fluids, **25**: 1409–1420 (1997).

No. of Figures: 11 No. of Tables: 01 No. of References: 18.

KEY WORDS: vortex shedding; shear flow; Strouhal number; square cylinder;

1. INTRODUCTION

The flow past bluff structures is a classic and important problem in fluid mechanics. It is frequently associated with periodic vortex shedding, causing dynamic forces on the structures. The velocity of the approaching stream may vary in the direction normal to a generator of the body. A typical relevant case might be that of a long-span structure such as a suspension bridge or a pipeline system which is parallel to the ground or water surface present in the planetary boundary layer. In the consideration of the shearing effect an important variation of the basic flow is the situation where the incoming freestream is a uniform shear flow. It is obviously implied that a constant vorticity and energy production are embedded in the freestream and this gives rise to complicated interations associated with flow separations. Therefore it is important to understand the mechanism of vortex shedding behind the bluff body under the effect of the presence of shear in the approaching stream.

The problem of vortex shedding behind a rectangular cylinder in uniform flows has recently been

*Correspondence to: R. R. Hwang, Institute of Physics, Academia Sinica, Nankang, Taipei 11529, Taiwan.
Contract grant sponsor: National Science Council, Taiwan; Contract grant number NSC85-2611-E-001-003.
Contract grant sponsor: Instritute of Physics, Academia Simica, Taiwan.

CCC 0271–2091/97/121409–12 $17.50

Received May 1996
Revised February 1997

investigated both numerically and experimentally by many researchers.[1–5] Patankar and Kelkar[6] also investigated the onset of vortex shedding by means of a linear stability analysis of the steady flow. The structure of vortex shedding behind a square cylinder in a channel was recently investigated numerically by Davis *et al.*[7] and Biswas *et al.*[8] to study the effect of the wall on the flow characteristics of vortex shedding.

The effect of freestream shear on the formation of the wake, the vortex-shedding mechanism, etc., on the other hand, is a topic of recent origin. Kiya *et al.*[9] and Sung and Hgun[10] investigated experimentally the vortex shedding from a circular cylinder in moderate-Reynolds-number shear flows. Ayukawa *et al.*[11] conducted a theoretical and experimental study on the effect of shear rate on the Strouhal number for a square cylinder in a uniform shear flow. In Ayukawa *et al.*'s simulation the flow is assumed to be the superposition of a potential flow which consists of a system of vortex filaments representing approximately the square cylinder. No Reynolds number variation was considered in their study.

It is expected that the shear rate influences not only the vortex shedding but also the flow pattern in the wake of the cylinder, which causes environmental disturbance downstream of a large structure. The purpose of this study is to investigate the effects of various shear strengths and Reynolds numbers on the periodic shedding motion behind a square cylinder by solving the full Navier–Stokes equations with numerical techniques. The advantage of a numerical simulation is the accessibility of a detailed analysis and nuances of flow development. Two parameters usually govern the uniform flow—one is the shear strength and the other is the Reynolds number. The aim of the present study is to investigate the influence of these parameters on the frequency of vortex shedding and the aerodynamic forces acting on the square cylinder.

2. STATEMENT OF PROBLEM

The physical problem considered in this study is a two-dimensional, viscous, incompressible flow around a square cylinder placed in a uniform shear flow. Figure 1 shows the geometry and co-ordinates of the flow problem. Far upstream of the cylinder the approaching stream is assumed to have a linear shear velocity

$$u = U_0 + Gy, \tag{1}$$

in which U_0 is the speed of the undisturbed stream at the centre of the cylinder and G is the transverse velocity gradient of the shear flow. By defining a length B, the width of the cylinder, and the velocity U as characteristic parameters, the governing equations for continuity and momentum may be expressed in the dimensionless conservative form

$$D = \frac{\partial u}{\partial x} + \frac{\partial v}{\partial y} = 0, \tag{2}$$

$$\frac{\partial u}{\partial t} + \frac{\partial}{\partial x}(u^2) + \frac{\partial}{\partial y}(uv) = -\frac{\partial p}{\partial x} + \frac{1}{Re}\left(\frac{\partial^2 u}{\partial x^2} + \frac{\partial^2 u}{\partial y^2}\right), \tag{3}$$

$$\frac{\partial v}{\partial t} + \frac{\partial}{\partial x}(uv) + \frac{\partial}{\partial y}(v^2) = -\frac{\partial p}{\partial y} + \frac{1}{Re}\left(\frac{\partial^2 v}{\partial x^2} + \frac{\partial^2 v}{\partial y^2}\right). \tag{4}$$

Here x and y are the co-ordinates of a fixed Cartesian system, t is the dimensionless time, u and v are the dimensionless velocity components in the x- and y-direction respectively, $p = P/\rho U_0^2$ is the dimensionless pressure and $Re = U_0 B/v$ is the Reynolds number.

In order to make the problem computationally feasible, artificial confining boundaries are placed sufficiently far from the body so that their presence has little effect on the characteristics of the flow

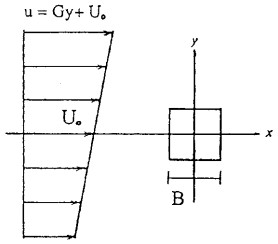

Figure 1. Considered flow problem

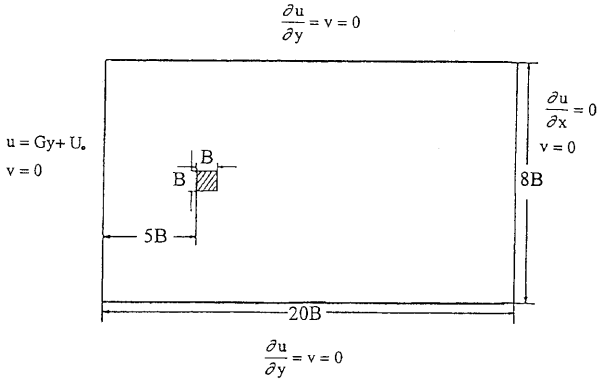

Figure 2. Computational domain and boundary conditions for considered flow

near the square cylinder. Figure 2 shows the computational domain. The governing equations (2)–(4) subject to the appropriate boundary conditions are to be solved by an appropriate numerical technique. The boundary conditions of interest in this study are as follows.

At the top and bottom boundaries of the domain,

$$\frac{\partial u}{\partial y} = v = 0. \tag{5}$$

At the entrance to the domain a uniform shear flow condition given by equation (1) has been employed. At the exit from the domain a Neumann-type boundary condition is used by setting

$$\frac{\partial u}{\partial x} = \frac{\partial v}{\partial x} = 0. \tag{6}$$

This ensures smooth transition through the outlet. No-slip boundary conditions for the velocities on the square cylinder are used.

3. METHOD OF SOLUTION

A modified version of the marker-and-cell (MAC) method[13] is used to obtain the numerical solution of equations (2)–(4). The computational domain is divided into Cartesian cells are shown in Figure 3. Staggered grid arrangements are used in which velocity components are defined at the midpoints of the cell sides to which they are normal. The pressure is defined at the centre of the cell as shown in Figure 4.

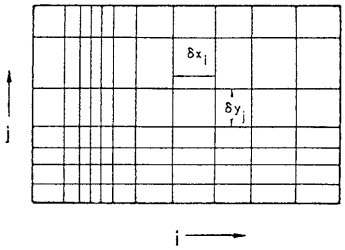

Figure 3. Finite difference mesh with variable rectangular cells

A time-dependent solution is obtained by advancing the flow field variables through a sequence of short time steps of duration δt. The advancement for one time step is calculated in two stages. First the velocity components are all advanced using the previous state of the flow to calculate the accelerations caused by convection, viscous stress, pressure gradients, etc. In other words, stage one consists of a single explicit calculation. However, this explicit time advancement does not necessarily lead to a velocity field with zero divergence. Thus, in stage two, adjustments must be made to ensure mass conservation. This is done by adjusting the pressure in each cell in such a way that there is no net mass flow into or out of the cell. A change in one cell will affect neighbouring cells, so this pressure adjustment must be performed iteratively until all cells have simultaneously achieved a zero mass change. This iterative correction of explicitly advanced velocity fields through an implicit continuity equation is equivalent to the solution of a Poisson equation for pressure.[12] In the iterative pressure–velocity correction process the overrelaxation factor is chosen as 1·8. Iterations continue until the divergence-free velocity field is obtained. However, for this purpose the divergence D in each cell is brought below a preassigned small value ε. In the present case ε is typically 10^{-5}.

In the original SOLA method the convective terms are modelled by a weighted average of upwind and central differencing[13] which is controlled by a weighting factor. The general form at $(i+\frac{1}{2}, j)$ is

$$\text{fux} = (u_{i+1/2,j}/\delta x_\alpha)[\delta x_{i+1}\text{DUL} + \delta x_i \text{DUR} + \theta\,\text{sgn}(u)(\delta x_{i+1}\text{DUL} - \delta x_i \text{DUR})], \tag{7}$$

where

$$\text{DUL} = (u_{i+1/2,j} - u_{i-1/2,j})/\delta x_i, \qquad \text{DUR} = (u_{i+3/2,j} - u_{i+1/2,j})/\delta x_{i+1},$$
$$\delta x_\alpha = \delta x_{i+1} + \delta x_i + \theta\,\text{sgn}(u)(\delta x_{i+1} - \delta x_i)$$

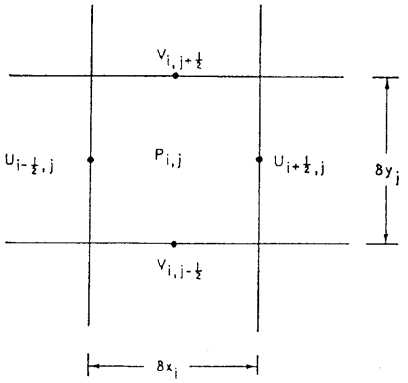

Figure 4. Location of variables in typical mesh cell

and sgn(u) means the sign of $u_{i+1/2,j}$. When $\theta = 0$, this approximation reduces to a second-order-accurate centred difference approximation. When $\theta = 1$, the first-order upwind is recovered. It was found that the simulation was strongly dependent on the weighting factor[1] and thus it was decided to utilize the higher-order QUICK scheme.[14] It has been proved that Leonard's scheme no longer has third-order accuracy when applied to non-uniform grids and can have large errors when grid non-uniformity becomes important.[15] In this study we thus use a counterpart of the QUICK scheme which is suitable for non-uniform grids.[15] For $u_{i+1/2,j} > 0$,

$$\text{fux} = u_{i+1/2,j}(\alpha u_{i-3/2,j} + \beta u_{i-1/2,j} - (\alpha + \beta + \gamma)u_{i+1/2,j} + \gamma u_{i+3/2,j}], \tag{8}$$

where

$$\alpha = \frac{ab}{c(c+a)(c-b)}, \qquad \beta = \frac{ac}{b(b+a)(b-c)}, \qquad \gamma = \frac{bc}{a(a+b)(a+c)},$$
$$a = \delta x_{i+1}, \qquad b = \delta x_i, \qquad c = \delta x_i + \delta x_{i-1}.$$

For uniform grids with $c/2 = a = b = \delta x$ the coefficients are the same as in QUICK. This type of approximation is used for all convective terms appearing in equations (3) and (4). Viscous diffusion terms are approximated with standard centred approximations.

The conditions necessary to prevent numerical instabilities are determined from the Courant–Friedrichs–Lewy (CFL) condition and the restriction on the grid Fourier numbers. First, material cannot move through more than one cell in one time step, because the difference equations assume fluxes only between adjacent cells. Therefore the time increment must satisfy the inequality

$$\delta t < \min\left\{\frac{\delta x_i}{|u_{i,j}|}, \frac{\delta y_j}{|v_{i,j}|}\right\}, \tag{9}$$

where the minimum is with respect to every cell in the mesh. Typically, δt is chosen equal to one-fourth to one-third of the minimum cell transit time. Second, when a non-zero value of kinematic viscosity is used, momentum must not diffuse more than approximately one cell in one time step. A linear stability analysis shows that this limitation implies

$$v\delta t < \frac{1}{2}\frac{\delta x_i^2 \delta y_j^2}{2\delta x_i^2 + \delta y_j^2}. \tag{10}$$

A somewhat more detailed description of the present solution algorithm has been discussed elsewhere.[16] The computations have been performed on a CONVEX-C3420 and HP-735 system.

4. RESULTS AND DISCUSSION

For the present computations 120×110 and 180×160 grids have been used. The grid is finer near the surfaces of the square cylinder to better resolve the gradients near the wall. The first point at a distance from each wall is $0{\cdot}01B$. The computational results for 120×110 and 180×160 grids show an average difference of $1{\cdot}5\%$ in the average drag coefficient for uniform flow at $Re = 500$. However, the computational time with 180×160 grids is much longer than with 120×110 grids. It can thus be said that for most practical purposes 120×110 grids can produce grid-independence results.

In order to assess the accuracy of the numerical computation of the present study, the case of a uniform flow past a square cylinder was computed for $\text{Re} = 500$, 1100 and 1500 and compared with previous studies. In Figure 5(a) we compare the variation in Strouhal number with Reynolds number with experimental data of Okajima.[3] Figure 5(b) is the computed average drag coefficient $\bar{C}_D$ compared with some predicted results of Davis and Moore,[1] Arnal *et al.*[17] and Li and Humphrey.[18]

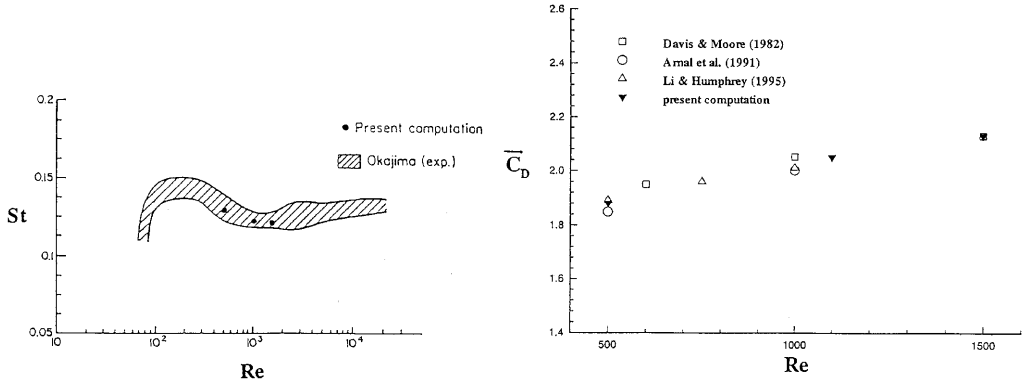

Figure 5. Comparison among (a) Strouhal number (St) and (b) drag coefficient ($\bar{C}_D$) results for flow past a square cylinder in a freestream

The computed Strouhal numbers of this study fall within the experimental results of Okajima. The computed average drag coefficients are also in close agreement with numerical results of previous studies. We then use the present numerical model to simulate the uniform shear flow over a square cylinder.

There are two non-dimensional parameters which govern the flow around a square cylinder in a uniform shear flow, i.e. the Reynolds number Re and the shear parameter K which are defined by $Re = U_0B/v$ and $K = GB/U_0$ respectively, where v is the kinematic viscosity of the fluid. The shear parameter can be interpreted as the non-dimensional vorticity of the shear flow. Computations have been carried out for flow over a rectangular cylinder in a uniform shear flow for various combinations of the parameter Re and K.

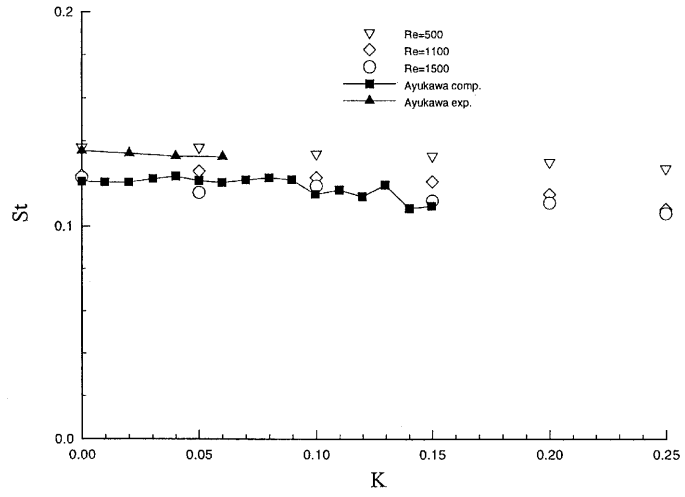

Figure 6. Variation in Strouhal number with shear rate at different Reynolds numbers

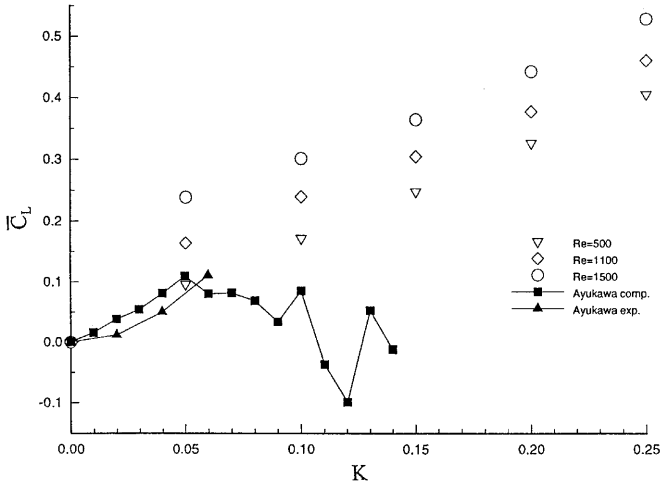

Figure 7. Effect of shear rate on mean lift coefficient at different Reynolds numbers

The effect of the shear rate G on the flow development behind a square cylinder was investigated via the shear parameter K defined by GB/U_0. All the results in the numerical calculations were obtained in the range of the stationary periodic flow pattern. In order to compare the computed results with the existing experimental data and theoretical study,[11] the calculated Strouhal number St, representing a frequency f of the periodic flow pattern, defined by fB/U_0 was obtained in relation to the shear parameter K and is shown in Figure 6. Since the simulation of Ayukawa *et al.*[11] used the discrete vortex model of the superposition of a potential flow, no Reynolds number was quoted in their study. Compared with the present study, their theoretical results coincided with the high Reynolds number $Re = 1500$, while the experimental results are in fairly good agreement with the case of $Re = 500$. The Strouhal number tends to decrease as the shear rate increases, but shows no

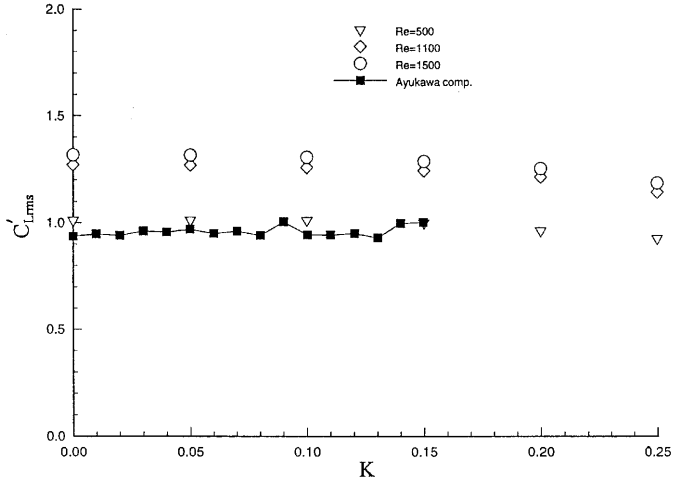

Figure 8. Effect of shear rate on RMS value of fluctuation of lift coefficient at different Reynolds numbers

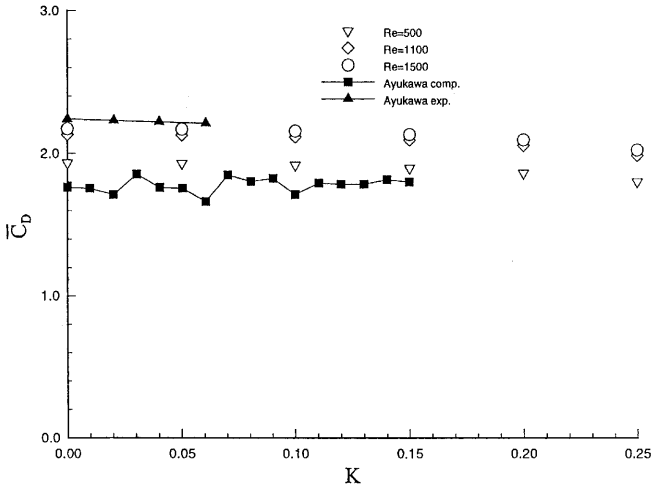

Figure 9. Effect of shear rate on mean drag coefficient at different Reynolds numbers

significant change at low shear rate. On the other hand, the Strouhal number decreases clearly as the Reynolds number increases.

Accompanying the periodic motion of the flow pattern, oscillation occurred in the lift on the square cylinder at the same frequency as the fluctuation of the flow motion. The amplitude of the fluctuation of lift was fairly large compared with the mean lift in the shear flow. Figures 7 and 8 show the effect of the shear parameter on the mean and RMS lift coefficients $\bar{C}_L$ and C'_{Lrms} respectively. Results of Ayukawa *et al.*'s study are also included for comparison. The mean lift coefficient increases sharply as the shear rate increases, in good agreement with the experiments. The simulation of Ayukawa *et al.* indicated that the change in mean lift coefficient, performing an irregular oscillation at high shear parameter, seems to be incorrect. The RMS lift coefficient tends to decrease as the shear rate increases at high shear rate and it increases its fluctuation with increasing Reynolds number.

The drag coefficient C_D, defined similarly to the lift coefficient as $F/\frac{1}{2}\rho U_2^0 A$, fluctuates much less than the lift coefficient, though a marked oscillation appears at high shear rate. The mean drag

Table I. Effect of freestream shearing on Strouhal number, drag and lift

	K	St	C_D	C_{Drms}	C_{Lrms}	C_L
$Re=500$	0·00	0·137	1·884	0·030	1·011	0·000
	0·05	0·137	1·880	0·034	1·013	0·096
	0·15	0·133	1·867	0·056	1·000	0·248
	0·25	0·127	1·801	0·092	0·926	0·405
$Re=1100$	0·00	0·124	2·052	0·036	1·271	0·000
	0·05	0·126	2·048	0·038	1·269	0·164
	0·15	0·121	2·013	0·041	1·243	0·305
	0·25	0·108	1·983	0·086	1·143	0·460
$Re=1500$	0·00	0·123	2·134	0·040	1·317	0·000
	0·05	0·116	2·130	0·047	1·316	0·239
	0·15	0·112	2·093	0·062	1·287	0·365
	0·25	0·106	2·022	0·083	1·186	0·528

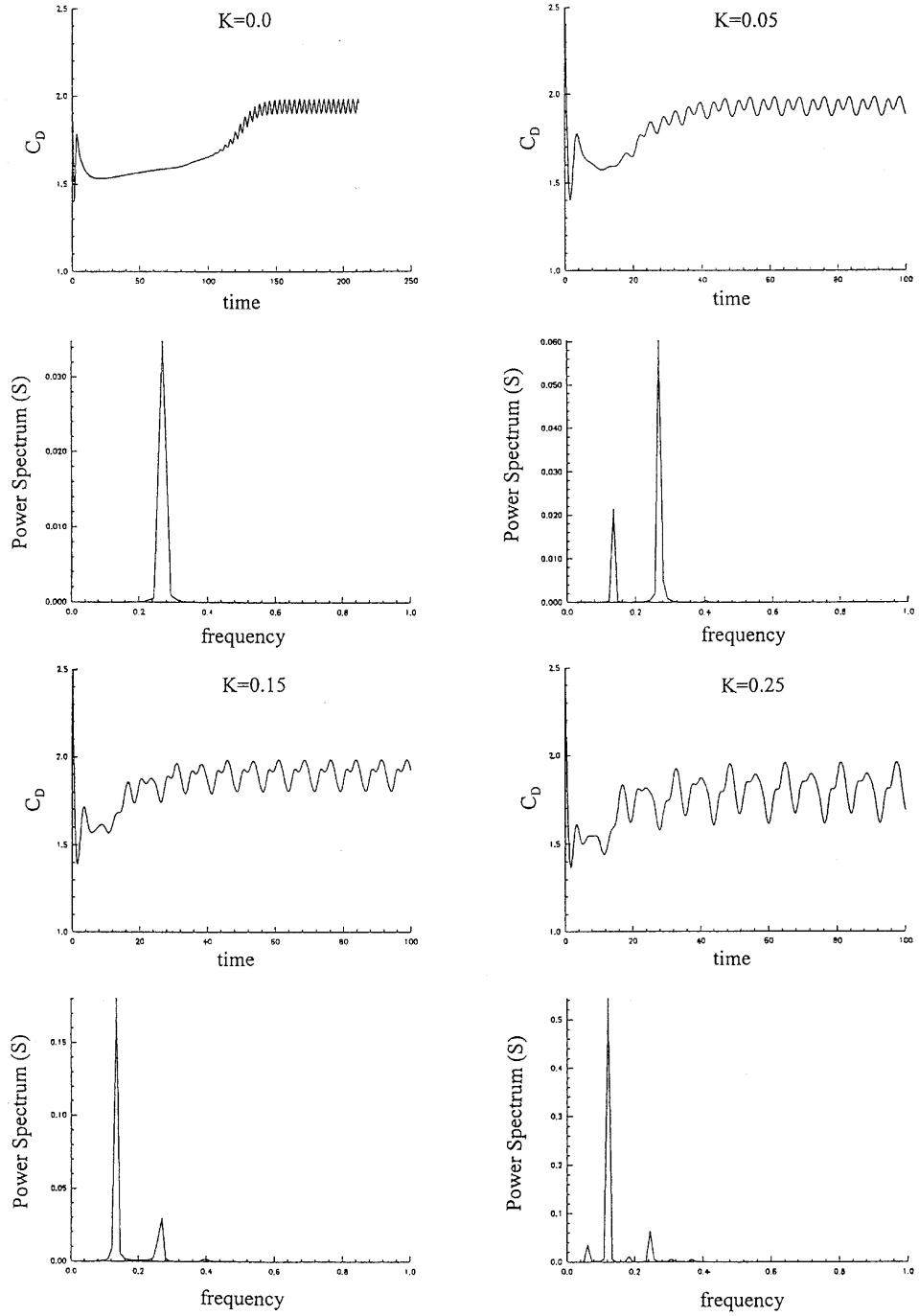

Figure 10. Time history of drag coefficient and its fluctuating spectrum for various shear rates at $Re = 500$

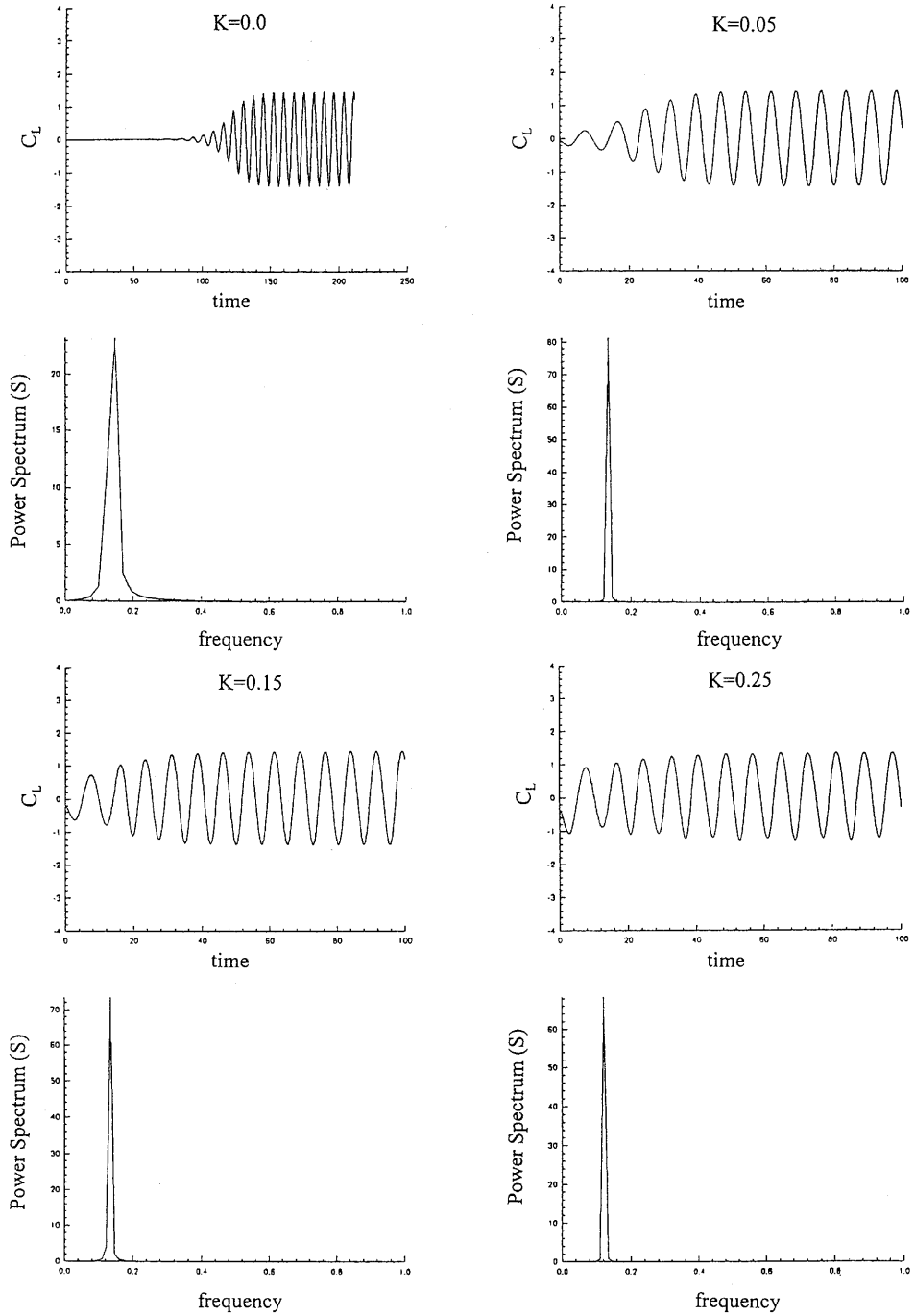

Figure 11. Time history of lift coefficient and its fluctuating spectrum for various shear rates at $Re = 500$

coefficient $\bar{C}_D$ is shown in Figure 9. It is in good agreement with the experiments at high Reynolds number. The mean drag coefficient decreases as the shear rate increases at high shear parameter, but the change is fairly small at low shear parameter. With increasing Reynolds number of the flow the mean drag coefficient is seen to increase within the extent of our simulation. Table I gives the Strouhal number and the average and RMS values of lift and drag coefficients for different shear parameters at various Reynolds numbers.

Figures 10 and 11 show the computed histories of instantaneous drag and lift coefficients with their corresponding power spectra of fluctuation, S, respectively for various shear parameters at $Re = 500$. In shear flow the asymmetry of the freestream excites the fluctuation motion of the vortex wake and causes the onset of vortex shedding to occur earlier than for a uniform stream. In the case of uniform flow ($K = 0$), one harmonic oscillation exists for both instantaneous drag and lift coefficients in the vortex-shedding motion, and the frequency of the fluctuation of C_D is nearly twice that of C_L. For shear flow ($K \neq 0$), although the fluctuating lift coefficient still has one harmonic like that for $K = 0$, a subharmonic has entered into the fluctuation of C_D. The strength of the subharmonic increases as the shear rate increases, and the fluctuation frequencies of C_L and C_D become identical at $K \geqslant 0{\cdot}15$.

5. CONCLUSIONS

With the numerical simulation of a finite difference method, the unsteady flow pattern around a square cylinder in a uniform shear flow was successfully obtained. The effect of shear rate on the cylinder tends to reduce the oscillation of the vortex wake behind the cylinder as the shear rate increases. The Strouhal number, mean drag and RMS lift coefficients tend to decrease as the shear rate increases, but show no significant change at low shear parameter. The mean lift shows a clear increase with increasing shear rate. Owing to the shear rate effect of the freestream, a subharmonic is induced in the fluctuation of drag force and its strength increases as the shear rate increases. For a shear parameter $K \geqslant 0{\cdot}15$ the frequencies of the fluctuating lift and drag coefficients become the same.

ACKNOWLEDGEMENTS

This work was supported by the National Science Council, Taiwan under grant NSC85-2611-E-001-003 and by the Institute of Physics, Academia Sinica, Taiwan.

REFERENCES

1. R. W. Davis and E. F. Moore, 'A numerical study of vortex shedding from rectangles', *J. Fluid Mech.*, **116**, 475–506 (1982).
2. R. Franke, W. Rodi and B. Schoenung, 'Numerical calculation of laminar vortes shedding flow past cylinders', *J. Wind Engng. Ind. Aerodyn.*, **35**, 237–257 (1990).
3. A. Okajima, 'Strouhal numbers of rectangular cylinders', *J. Fluid Mech.*, **123**, 379–398 (1982).
4. A. Okajima, 'Numerical simulation of flow around rectangular cylinders', *J. Wind Engng. Ind. Aeordyn.*, **33**, 171–180 (1990).
5. A. Okajima and H. Sakai, 'Numerical simulation of laminar and turbulent flows around rectangular cylinders', *Int. j. numer. meth. fluids*, **15**, 999–1012 (1992).
6. S. V. Patankar and K. M. Kelkar, 'Numerical prediction of vortex shedding behind a square cylinder', *Int. j. numer. meth. fluids*, **14**, 327–341 (1992).
7. R. W. Davis, E. F. Moore and L. P. Purtell, 'A numerical–experimental study of confined flow rectangular cylinders', *Phys. Fluids*, **27**, 46–59 (1984).
8. G. Biswas, A. Mukhopadhyay and T. Sindararajan, 'Numerical investigation of confined wakes behind a square cylinder in a channel', *Int. j. numer. meth. fluids*, **14**, 1473–1484 (1992).
9. M. Kiya, H. Tamura and M. Arie, 'Vortex shedding from a circular cylinder in moderate-Reynolds-number shear flow', *J. Fluid Mech.*, **141**, 721–735 (1980).

10. H. J. Sung and J. M. Hyun, 'Experimental investigation of uniform-shear flow past a circular cylinder', *J. Fluids Engng.*, **114**, 457–460 (1992).
11. K. Ayukawa, J. Ochi, G. Kawahara and T. Hirao, 'Effects of shear rate on the flow around a square cylinder in a uniform shear flow', *J. Wind Engng. Ind. Aerodyn.*, **50**, 97–106 (1993).
12. J. A. Viecelli, 'A computing method for incompressible flows bounded by moving walls', *J. Comput. Phys.*, **8**, 119–143 (1971).
13. C. W. Hirt, B. D. Nichols and N. C. Romero, 'SOLA—A numerical solution algorithm for transient fluid flows', *Los Alamos Scientific Laboratory Report LA-5852*, 1975.
14. B. P. Leonard, 'A stable and accurate convective modeling procedure based on quadratic upstream interpolation', *Comput. Meth. Appl. Mech. Engng.*, **19**, 59 (1979).
15. J. Liu, G. A. Pope and K. Sepehrnoori, 'A high-resolution finite-difference scheme for nonuniform grids', *Appl. Math. Model.*, **19**, 162 (1995).
16. B. D. Nichols, C. W. Hirt and R. S. Hotchkiss, 'SOLA-VOF: a solution algorithm for transient fluid flow with multiple free-boundaries', *Los Alamos Scientific Laboratory Rep. LA-8355*, 1980.
17. M. P. Arnal, D. J. Goering and J. A. C. Humphrey, 'Vortex shedding from a bluff body on a sliding wall', *J. Fluids Engng.*, **113**, 384–398 (1991).
18. G. Li and J. A. C. Humphrey, 'Numerical modelling of confined flow past a cylinder of square cross-section at various orientations', *Int. j. numer. meth. fluids*, **20**, 1215–1236 (1995).

